

CONSTRAINTS ON THE PROPER MOTION OF THE ANDROMEDA GALAXY BASED ON THE SURVIVAL OF ITS SATELLITE M33

ABRAHAM LOEB, MARK J. REID

Harvard-Smithsonian Center for Astrophysics, 60 Garden Street, Cambridge, MA 02138, USA

ANDREAS BRUNTHALER

Joint Institute for VLBI in Europe, Postbus 2, 7990 AA Dwingeloo, The Netherlands

HEINO FALCKE

ASTRON, Postbus 2, 7990 AA Dwingeloo, The Netherlands

Department of Astrophysics, Radboud Universiteit Nijmegen, Postbus 9010, 6500 GL Nijmegen,
The Netherlands

Draft version October 25, 2018

ABSTRACT

A major uncertainty in the dynamical history of the local group of galaxies originates from the unknown transverse speed of the Andromeda galaxy (M31) relative to the Milky Way. We show that the recent VLBA measurement of the proper motion of Andromeda's satellite, M33, severely constrains the possible values of M31's proper motion. The condition that M33's stellar disk will not be tidally disrupted by either M31 or the Milky Way over the past 10 billion years, favors a proper motion amplitude of $100 \pm 20 \text{ km s}^{-1}$ for M31 with the quadrant of a negative velocity component along Right Ascension and a positive component along Declination strongly ruled-out. This inference can be tested by future astrometric measurements with SIM, GAIA, or the SKA. Our results imply that the dark halos of Andromeda and the Milky Way will pass through each other within the next 5–10 billion years.

1. INTRODUCTION

The local group of galaxies provides the nearest laboratory for the dynamics and evolution of galaxies. Its two dominant galaxies, the Milky Way and Andromeda (M31) are separated by a distance of $\sim 700 \text{ kpc}$ and are moving towards each other with a radial velocity of -117 km s^{-1} (Binney & Tremaine 1987). The unknown transverse velocity of M31 relative to the Milky Way introduces an ambiguity into the dynamical history of the local group and the likely dark-matter mass of its components (Peebles 1995; Peebles et al. 2001). The system potentially provides a local example for the dynamics that leads more generally to the formation of elliptical galaxies out of the merger of two disks (Barnes 1998).

The estimated ages of stars within the disks of the Milky Way and Andromeda imply that these disks formed ~ 10 billion years ago, and their small scale height suggests that they had not experienced any substantial merger activity since then (Wyse 2000; Gilmore, Wyse, & Norris 2002; Peloso, da Silva, & Arani-Prado 2005; Toth & Ostriker 1992).

Recent VLBA observations of two H₂O masers on opposite sides of Andromeda's satellite, M33, led to a geometric determination of its distance $730 \pm 168 \text{ kpc}$ and total velocity of $190 \pm 59 \text{ km s}^{-1}$ relative to the Milky Way (Brunthaler et al. 2005). Unfortunately, no such masers were found in Andromeda, despite extensive search efforts (e.g. Imai et al. 2001). M33 has a thin H I/stellar disk that extends out to a radius of $\sim 10 \text{ kpc}$ (Corbelli & Schneider 1997). Here we use the existence of this disk and its measured position and bulk velocity in three-dimensions, to constrain the transverse velocity of Andromeda. In particular, we use the constraints that: (i) M33's stellar disk was not disrupted by tidal interactions with the Milky Way and Andromeda over the past 10 billion years; and (ii) these

galaxies were closer to each other more than 10 billion years ago as participants in the expansion of the universe. In §2 we describe our prescription for the mass profiles of the galaxy halos under consideration and in §3 we present our numerical results. Finally, §4 summarizes our main conclusions.

2. HALO MASS PROFILES

We would like to constrain the velocity vector of M31 based on the condition that the stellar disk of M33 (as represented by test particles on circular orbits at radii $\lesssim 10 \text{ kpc}$ from the center of M33) was not disrupted during the past ~ 10 billion years. For simplicity, we assume a spherical distribution of enclosed mass, $M(r)$, within each of the galaxy halos under consideration (M31, M33, and the Milky Way) and follow orbits of test particles in them. In order to solve for the orbits of these test particles we only need to specify the gravitational acceleration as a function of radial distance r from the center of these halos, $\vec{g} = g_r(r)\hat{e}_r$, where

$$g_r = -\frac{GM(r)}{r^2} = -\frac{v^2(r)}{r}, \quad (1)$$

with $v(r)$ being the circular velocity as function of radius within these halos.

Our test-particle approach ignores the effect of dynamical friction on the orbit of M33 inside the halo of M31. The additional effect of dynamical friction can only strengthen our constraints since it would bring M33 closer to the core of M31, where it would be more vulnerable to tidal disruption. Hence, our simple test-particle approach provides conservative constraints on the allowed range of possible orbits for the M33/M31 system. For an elaborate discussion on the impact of dynamical friction on the survival of satellite halos, see Taffoni et al. (2003) and references therein.

The simplest model of galaxy halos assumes a flat rotation curve, $v = \text{const}$, out to a truncation radius r_t . Since all three galaxies under consideration have H I disks, the values of v can be inferred from their corresponding kinematic data, namely ~ 110 , 220 , and 250 km s $^{-1}$ for M33, the Milky Way, and M31, respectively. The truncation radius is related to the total mass of the halo, M_t , through the expression $r_t = GM_t/v^2$. For M33, r_t is dictated by the tidal effect of M31. Given an orbit of M33, we find r_t for M33 by searching for the largest radius at which a test particle initially on a circular orbit around M33 would remain bound to it.

For M31 and the Milky Way, it is natural to associate r_t with the virial radius, r_v , inside of which the mean halo density is ~ 200 times larger than the mean density of the universe when these galaxies formed. More precisely, in a flat universe with density parameters Ω_m in matter and $\Omega_\Lambda = 1 - \Omega_m$ in a cosmological constant, the density of the halo in units of the critical density at the collapse redshift z of the halo is (see §2.3 in Barkana & Loeb 2001 for more details),

$$\Delta_c = 18\pi^2 + 82d - 39d^2, \quad (2)$$

where $d = \Omega_m^z - 1$ and

$$\Omega_m^z = \frac{\Omega_m(1+z)^3}{\Omega_m(1+z)^3 + \Omega_\Lambda}. \quad (3)$$

A halo of virial mass M_v that formed at a redshift z has a physical virial radius of

$$r_v = 84.5 \times M_{12}^{1/3} [f(z)]^{-1/3} \left(\frac{1+z}{2} \right)^{-1} h^{-1} \text{kpc}, \quad (4)$$

and a corresponding circular velocity at the virial radius,

$$v_v = 225.5 \times M_{12}^{1/3} [f(z)]^{1/6} \left(\frac{1+z}{2} \right)^{1/2} \text{km s}^{-1}. \quad (5)$$

Here $M_{12} \equiv (M_v/10^{12} h^{-1} M_\odot)$, h is the present-day value of the Hubble constant in units of 100 km s $^{-1}$ Mpc $^{-1}$, and $f(z) \equiv [(\Omega_m/\Omega_m^z)(\Delta_c/18\pi^2)]$. Our choice for the virialization redshift of M31, M33, and the Milky Way is $z \sim 1$ (Wyse 2000; Gilmore, Wyse, & Norris 2002). Nuclear dating of the thin Galactic disk implies an age of $\sim 8.3 \pm 1.8$ Gyr corresponding to a formation redshift $z \sim 1$ (Peloso et al. 2005), as expected from other considerations for spiral galaxies (Hammer et al. 2005). The total halo masses of the Milky Way and M31 were also constrained directly in the literature (Binney & Tremaine 1987; Gottesman, Hunter, & Boonyasait 2002; Battaglia et al. 2005). We parametrize the masses of M31 and the Milky Way in units of 3.4 and $2.3 \times 10^{12} M_\odot$ respectively, and adopt the WMAP values for the cosmological parameters, namely $\Omega_m = 0.27$, $\Omega_\Lambda = 1 - \Omega_m = 0.73$, and $h = 0.71$ (Spergel et al. 2003).

To refine our constraints, we adopt a halo profile that follows from cosmological simulations of galaxy formation. Navarro, Frenk, & White (1997; hereafter NFW) found an analytic fit to results from their cosmological N-body simulations of galaxy halos in a cold dark matter cosmology. The density profile in their model has an asymptotic radial dependence of r^{-3} at large distances and r^{-1} at small distances. The model has two free parameters: one is the transition radius that separates these different power-law

dependencies, r_s , and the second is the so-called “concentration parameter”, c , which denotes the ratio between the virial radius r_v and r_s .

The radial gravitational acceleration in the NFW model is given by

$$g_r = -\frac{GM_v}{r^2} \frac{\ln(1+cx) - (cx)/(1+cx)}{[\ln(1+c) - c/(1+c)]} \quad (6)$$

where $x = r/r_v$ with r_v given by equation (4). The present-day concentration parameter is correlated with the halo collapse redshift (Wechsler et al. 2002).

3. NUMERICAL RESULTS

Our goal is to examine a wide range of trial proper motions for M31, compute the history of the M33/M31/Milky Way system, and determine which proper motions lead to the survival of M33’s stellar disk. Our numerical simulations used S. Aarseth’s NBODY0 code¹, modified to allow the extended dark-matter potentials associated with the galaxies. M31 and the Milky Way were treated as extended rigid bodies while the disk and halo of M33 were modelled as a collection of test particles moving in the combined, time-dependent potential of M31, the Milky Way, and M33. We used a Galactic Cartesian coordinate system in which the Milky Way is in the (x, y) plane, with the Galactic Center at $(8, 0, 0)$ kpc, y is toward Galactic rotation, and z is toward the North Galactic Pole.

The calculations were initialized to match today’s positions and motions of M33, M31, and the Milky Way. While we have a measured proper motion for M33, none exist for M31. Therefore, we assigned trial values for the proper motion for M31 in the eastward ($\alpha \cos \delta$) and northward (δ) directions and then converted them to the Galactic Cartesian frame. The observed radial velocity of M31 relative to the center of the Milky Way is -117 km s $^{-1}$, which converted to the Galactic Cartesian frame yields $(56, -93, 43)$ km s $^{-1}$. The radial and trial proper motions were combined to give the full velocity vector of M31 at the present epoch. For the distances of M31 and M33 from the Milky Way we adopt the respective values of 786 kpc and 794 kpc (McConnachie et al. 2004; 2005).

M31 and the Milky Way were assigned total masses of $3.4m_f$ and $2.3m_f \times 10^{12} M_\odot$ and truncation radii r_t of $235m_f$ and $207m_f$ kpc respectively (consistently with their measured rotation curves for the isothermal sphere model). The scaling parameter m_f was used to test the sensitivity of our results to the total dark matter masses (for recent empirical constraints, see Battaglia et al. (2005) and references therein). The dark matter distributions of M31 and the Milky Way were assigned an NFW halo mass profile with a concentration parameter $c = 11.9$ (Navarro, Frenk, & White 1997). Our results are not sensitive to reasonable variations in c . We also tested the truncated singular isothermal sphere as an alternative dark matter mass distribution and found that it produced similar, albeit slightly greater, tidal stripping and heating of M33.

The stellar disk of M33 at 10 or 5 Gyr ago was simulated with typically 100 collisionless particles uniformly placed between 2.5 and 7.5 kpc of the center of M33 in the (x, y) plane. The outer cutoff simulates approximately

¹ <http://bima.astro.umd.edu/nemo/>; see also <http://www.ast.cam.ac.uk/sverre/web/pages/home.htm>

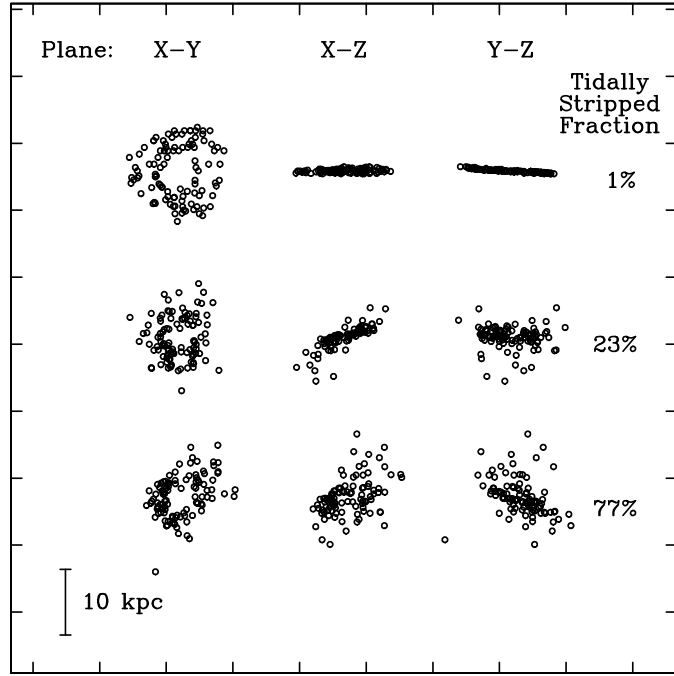


FIG. 1.— Three examples of tidal stripping and heating of the stellar disk of M33. The locations of stars at the end of the N-body simulation are shown projected onto three orthogonal planes, as labeled at the top of the figure. These examples all used the full dark matter halos ($m_f = 1$) and simulated histories over the past 10 Gyr. A 10 kpc scale is shown in the bottom left corner. *Top:* Simulation with $(V_{\alpha \cos \delta}, V_{\delta}) = (100, -100) \text{ km s}^{-1}$ for M31, which resulted in essentially no tidal stripping (tidally stripped fraction of $\sim 1\%$). *Middle:* Simulation with $(V_{\alpha \cos \delta}, V_{\delta}) = (-50, -50) \text{ km s}^{-1}$ for M31, which resulted in moderate tidal stripping (23%). *Bottom:* Simulation with $(V_{\alpha \cos \delta}, V_{\delta}) = (0, 0) \text{ km s}^{-1}$ for M31, which resulted in heavy tidal stripping and heating (77%).

the maximum extent of the stellar disk in M33 (Corbelli & Schneider 1997). The inner cutoff was adopted for computational speed; since tidal heating and stripping starts from the outside and proceeds inward, the fate of test stars near the center of M33 is of little interest for our purposes.

Since strong tidal stripping and heating of M33's halo is also a possibility, the dark matter distribution of M33 was monitored by placing roughly 100 “mass-tracing” particles at 1 kpc spacings out to the truncation radius of the galaxy. The enclosed mass profile for M33 was updated every 10^8 yr from the locations of the mass-tracing particles, azimuthally averaged and binned as a function of radius from the center of M33. As these mass-tracing particles interacted with M31 and the Milky Way, some were tidally stripped, steepening the fall-off of mass with radius in M33. The halo stripping and heating of M33 did not affect significantly its orbit (because of its low mass) but had some effect on the tidal disruption of its stellar disk. We therefore started the calculation by integrating the coordinates of the three galaxies backwards in time to obtain initial conditions either 10 or 5 Gyr ago. This was implemented by reversing the sign of today's velocity vector for each galaxy. With the entire system specified in the past, the calculation proceeded forward in time to the present epoch and included the stripping and heating of M33's dark halo and stellar disk.

Once the local group arrived at the present time, we displayed the locations of the “disk” stars in M33, as illustrated in Figure 1. In some trials, the disk stars remained in orbit about the center of M33 with little change in radial distribution or the original orbital plane, indicating little tidal stripping and heating. In other trials, many

stars were moved to much greater radii, the mean orbital plane was rotated and warped, and the distribution was more triaxial than planar, indicating strong tidal heating after a few passages near M33 or the Milky Way.

In order to evaluate quantitatively the degree of tidal stripping and heating, we produced a simple estimate of the percentage of stars “stripped” from M33. Stars moved to radii greater than 8 kpc or out of the initial stellar plane by more than 20% of their radial distance, were considered stripped. We determined the stellar plane in an approximate manner, by fitting straight lines to the projected distributions in the (x, z) and (y, z) planes, rotating the system back to the (x, y) plane, and calculating each star's distance from this plane (z -distance). In general, three Euler angles are needed to correct the rotation of a system. However, for small tidal rotations of the stellar plane, our procedure is adequate since we start with the stars in a plane aligned with the Cartesian axes. For large rotations ($\gtrsim 30^\circ$), we optimized this procedure by considering a 7×7 grid of rotation angles spaced by 7° and centered on the initial results; for each test we calculated the percentage of stripped stars and adopted the rotations that produced the minimum stripping.

Figure 2 displays the percentage of stars in M33 that were tidally stripped over a wide range of trial proper motions for M31. For the galaxy masses listed above and a lookback time of 10 Gyr, large areas of proper-motion space for M31 result in significant ($> 50\%$) tidal stripping of M33's stellar disk, including most proper motions smaller than $\sim 75 \text{ km s}^{-1}$. We repeated our calculations for two lookback times (5 or 10 Gyr) and for two estimates of total galaxy masses (given by m_f of 1.0 and 0.75). Re-

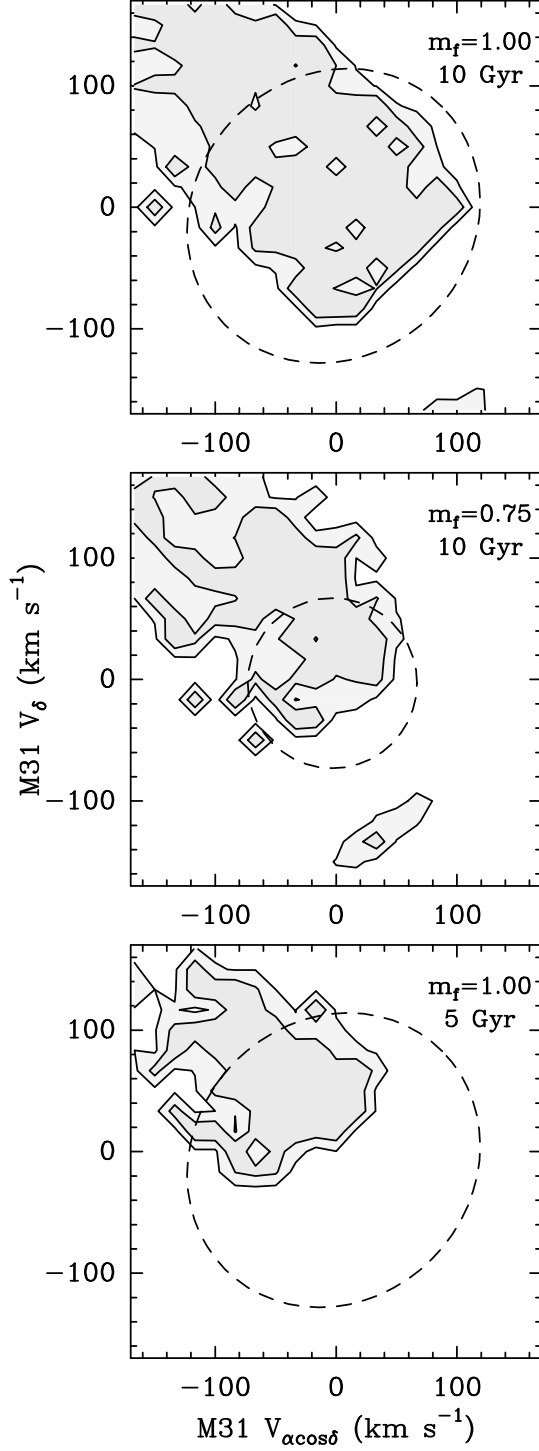


FIG. 2.— The fraction of tidally stripped stars as a function of the trial proper motion of M31. Trial proper motions are in Equatorial coordinates (Right Ascension, α , and Declination, δ). Contours delineate 20% (light grey) and 50% (dark grey) of the total number of stars stripped in the simulation. Regions inside the dashed ellipses correspond to trial proper motions that satisfy the condition that the separation between M31 and the Milky Way was smaller 10 Gyr ago than it is today (the “timing” argument). *Top:* Simulations with full dark matter halos ($m_f = 1$) and over the past 10 Gyr. The excluded region of proper motion is directed North-West. *Middle:* Simulations with reduced dark matter halos ($m_f = 0.75$) and over the past 10 Gyr. *Bottom:* Simulations with full dark matter halos ($m_f = 1$) and over the past 5 Gyr.

ducing either the lookback time or the masses of the galaxies reduces the stripping, although significant stripping and heating still occurs over large areas of proper-motion space for M31. Since the real M33 does not appear to have undergone significant tidal heating, the darkly shaded areas in Figure 2 would seem to be ruled out as possible

proper motions for M31.

We tested the sensitivity of our conclusions to uncertainties in M33’s proper motion, the relative distances of M31 and M33, and the initial orientation of the stellar disk in M33. In one test, shifting the motion of M33 by 70 km s^{-1} (randomly in the three Cartesian coordinates) increased

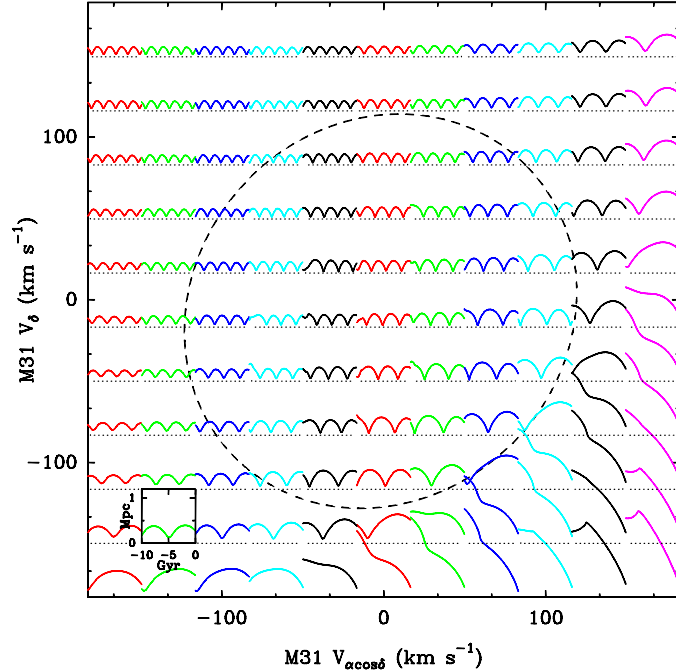


FIG. 3.— The separation between M33 and M31 as a function of lookback time for many trial proper motions of M31 (indicated the bounding axes). The scale for the individual plots is marked on the box near the lower left corner. The region inside the dashed ellipse corresponds to trial proper motions that satisfy the condition that the separation between M31 and the Milky Way was smaller 10 Gyr ago than it is today. All examples assume the full dark matter halos ($m_f = 1$).

the tidal stripping and heating by about 20%. Increasing (decreasing) the distance of M31 by 34 kpc [$\sim \sqrt{2}$ times the 1σ precision of the observations in McConnachie et al. (2004,2005)] also increased (decreased) the stripping by $\sim 20\%$. The conclusions of the paper would change significantly only if the distance to M31 is decreased by $\gtrsim 50$ kpc (or through a similar increase in M33’s distance, since the tidal effect depends primarily on the separation between M31 and M33). Finally, rotating the original stellar disk of M33 by 90° (from the (x, y) to the (x, z) plane) reduced the stripping and heating by about 30%. Overall, we conclude that our results are only sensitive at the level of tens of percent to uncertainties in the initial configuration of our simulations.

One other constraint on the proper motion of M31 results from the “timing” argument (Kahn & Woltjer 1959; Peebles et al. 2001). Because the Universe has expanded considerably over the past ~ 10 Gyr, galaxies (or protogalaxies) should have been closer together in the distant past than they are today. Any large proper motion for M31 violates this argument. Since our calculations produce a time history of the separation of M31 and the Milky Way, we plotted this separation as a function of time and determined the approximate range of M31 proper motions for which these galaxies were closer together 10 Gyr ago than today. The regions inside the dashed ellipses in Figure 2 indicate approximately the proper motions of M31 for which this occurs. For values of $m_f \leq 0.5$, we have found that M31 and the Milky Way were never closer together in the past than today, for any of our trial proper motions of M31. Since this violates the timing argument, we do not show values of $m_f \leq 0.5$ in Figure 2.

For the fiducial case of $m_f = 1$ and a lookback time of 10 Gyr (top panel), the allowed proper-motion param-

eter space delineates an annular arc ~ 40 km s^{-1} wide that starts near $V_{M31} \approx (-90, 0)$, goes counter clockwise through $(0, -100)$ and $(90, 0)$, to $(50, 80)$ km s^{-1} along Right Ascension and Declination. Additional small “islands” of moderate stripping and heating exist with smaller likelihood.

Figure 3 shows the separation between M33 and M31 as a function of lookback time for the various trial proper motions of M31. Since we initiate all orbits by integrating M33’s orbit back in time without stripping and then integrate these orbits forward in time with stripping, we lose time-reversal symmetry and so there is some variation in the final separation between M31 and M33 among the different cases. Throughout the entire range allowed by the timing argument (delineated by the dashed line), M33 orbits around M31 several times as expected from a gravitationally-bound satellite. The repeated encounters, while not disruptive in the allowed range of proper motions, might have still stripped material from the outskirts of M33 and could potentially account for the streams of H I gas (Braun & Thilker 2004; Thilker et al. 2004) and stars (Guhathakurta et al. 2005) that are observed in between the two galaxies today.

4. CONCLUSIONS

Figure 2 presents our limits on the proper motion of M31 based on the constraint that the thin stellar disk of M33 (simulated as an ensemble of collisionless test particles on circular orbits) was not tidally disrupted over the past 10^{10} years through its orbit within the local group. This constraint and the condition that M31 and the Milky Way galaxies were closer in the past, favors a proper motion amplitude of 100 ± 20 km s^{-1} for M31 with the quadrant of a negative velocity component along Right Ascen-

sion and a positive component along Declination strongly ruled-out. The orbital angular momentum associated with the allowed range of proper motions implies that the dark halos of Andromeda and the Milky Way will pass through each other within the next 5–10 billion years. The main uncertainty in our results involves the dark halo masses of the local group members (compare the top two panels in Fig. 2).

Our inference relies on the validity of various simplifying assumptions. For example, we simulated the dynamics of M33 without taking account of the full dark-matter distribution interior to the local group (including the mass in between the Milky Way and Andromeda). In addition, we have assumed that the tidal influence of external objects on the local group can be neglected, and we have ignored

the addition of mass to the local group through accretion and infall of external matter. Obviously, the Milky Way and the Andromeda galaxies grew hierarchically with cosmic time but the ages and low velocity dispersion of stars within their disks argue against major merging encounters over the past 10 billion years (Wyse 2000; Gilmore, Wyse, & Norris 2002). Our quantitative predictions provide an added incentive for future astrometric observatories such as SIM², GAIA³, or the SKA⁴, that will be able to test them (Shaya et al. 2003).

We thank Andy Gould and Robert Braun for useful comments. This work was supported in part by NASA grant NAG 5-13292, and by NSF grants AST-0071019, AST-0204514 (for A.L.).

REFERENCES

Barkana, R., & Loeb, A. 2001, *Phys. Rep.*, 349, 125; astro-ph/0010468

Barnes, J. E. 1998 in *Galaxies: Interactions and Induced Star Formation*, SAAS-FEE Advanced Course 26, Kennicutt, R.C., Schweizer, F., & Barnes, J.E.; D. Friedli, L. Martinet, & D. Pfenniger, eds. (Springer-Verlag: Berlin), pp. 275-394

Battaglia, G., Helmi, A., Morrison, H., Harding, P., Olszewski, E. W., Mateo, M., Freeman, K. C., Norris, J., & Shectman, S. A. 2005, MNRAS, submitted; astro-ph/0506102

Binney, J., & Tremaine, S. 1987, *Galactic Dynamics*, Princeton University Press: Princeton, p. 605

Braun, R., & Thilker, D. A. 2004, *A&A*, 417, 421

Brunthaler, A., Reid, M. J., Falcke, H., Greenhill, L. J., & Henkel, C. 2005, *Science*, 307, 1440

Corbelli, E., & Schneider, S. E. 1997, *ApJ*, 479, 244

del Peloso, E. F., da Silva, L., & Arany-Prado, L. I. 2005, *A& A*, 434, 301

Gilmore, G., Wyse, R. F. G., & Norris, J. E. 2002, *ApJ*, 574, L39

Gottesman, S. T., Hunter, J. H., & Boonyyasait, V. 2002, *MNRAS*, 337, 34

Guhathakurta, P. et al. 2005, *Nature*, submitted; astro-ph/0502366

Hammer, F., Flores, H., Elbaz, D., Zheng, X. Z., Liand, Y., & Cesarsky, C. 2005, *A & A*, 430, 115

Imai, H., Ishihara, Y., Kameya, O., & Nakai, N. 2001, *PASJ*, 53, 489

Kahn, F. D., & Woltjer, L. 1959, *ApJ*, 130, 705

McConnachie, A. W., Irwin, M. J., Ferguson, A. M. N., Ibata, R. A., Lewis, G. F., & Tanvir, N. 2004, *MNRAS*, 350, 243

McConnachie, A. W., Irwin, M. J., Ferguson, A. M. N., Ibata, R. A., Lewis, G. F., & Tanvir, N. 2005, *MNRAS*, 356, 979

Navarro, J. F., Frenk, C. S., & White, S. D. M. 1997, *ApJ*, 490, 493

Peebles, P. J. E. 1995, *ApJ*, 449, 52

Peebles, P. J. E., Phelps, S. D., Shaya, E. J., & Tully, R. B. 2001, *ApJ*, 554, 104

Shaya, E. J., Tully, R. B., Peebles, P. J. E., Tonry, J. L., Borne, K., Vogel, S. N., Nusser, A., & Zaritsky, D. 2003, *Proc. SPIE*, 4852, 120

Spergel, D. N., et al. 2003, *AJ Suppl.*, 148, 175

Taffoni, G., et al. 2003, *MNRAS*, 341, 434; astro-ph/0301271

Thilker, D. A., Braun, R., Walterbos, R. A. M., Corbelli, E., Lockman, F. J., Murphy, E., & Maddalena, R. 2004, *ApJ*, 601, L39

Toth, G., & Ostriker, J. P. 1992, *ApJ*, 389, 5

Wechsler, R. H., Bullock, J. S., Primack, J. R., Kravtsov, A. V., & Dekel, A. 2002, *ApJ*, 568, 52

Wyse, R. F. G. 2000, preprints astro-ph/0012270 and astro-ph/0204190

² http://planetquest.jpl.nasa.gov/SIM/sim_index.html

³ <http://sci.esa.int/science-e/www/area/index.cfm?fareaid=26>

⁴ <http://www.skatelescope.org/>